Hindawi
Shock and Vibration
Volume 2018, Article ID 8273469, 15 pages
https://doi.org/10.1155/2018/8273469

Research Article

A Lab-Scale Experiment Approach to the Measurement of Wall Pressure from Near-Field under Water Explosions by a Hopkinson Bar

Xiongwei Cui, Xiongliang Yao, and Yingyu Chen

College of Shipbuilding Engineering, Harbin Engineering University, Harbin 150001, China

Correspondence should be addressed to Xiongliang Yao; xiongliangyao@hrbeu.edu.cn

Received 21 April 2018; Revised 16 July 2018; Accepted 8 August 2018; Published 9 September 2018

Academic Editor: Mickaël Lallart

Copyright © 2018 Xiongwei Cui et al. This is an open access article distributed under the Creative Commons Attribution License, which permits unrestricted use, distribution, and reproduction in any medium, provided the original work is properly cited.

Direct measurement of the wall pressure loading subjected to the near-field underwater explosion is of great difficulty. In this article, an improved methodology and a lab-scale experimental system are proposed and manufactured to assess the wall pressure loading. In the methodology, a Hopkinson bar (HPB), used as the sensing element, is inserted through the hole drilled on the target plate and the bar's end face lies flush with the loaded face of the target plate to detect and record the pressure loading. Furthermore, two improvements have been made on this methodology to measure the wall pressure loading from a near-field underwater explosion. The first one is some waterproof units added to make it suitable for the underwater environment. The second one is a hard rubber cylinder placed at the distal end, and a pair of ropes taped on the HPB is used to pull the HPB against the cylinder hard to ensure the HPB's end face flushes with loaded face of the target plate during the bubble collapse. To validate the pressure measurement technique based on the HPB, an underwater explosion between two parallelly mounted circular target plates is used as the validating system. Based on the assumption that the shock wave pressure profiles at the two points on the two plates which are symmetrical to each other about the middle plane of symmetry are the same, it was found that the pressure obtained by the HPB was in excellent agreement with pressure transducer measurements, thus validating the proposed technique. To verify the capability of this improved methodology and experimental system, a series of minicharge underwater explosion experiments are conducted. From the recorded pressure-time profiles coupled with the underwater explosion evolution images captured by the HSV camera, the shock wave pressure loading and bubble-jet pressure loadings are captured in detail at 5 mm, 10 mm, . . ., 30 mm stand-off distances. Part of the pressure loading of the experiment at 35 mm stand-off distance is recorded, which is still of great help and significance for engineers. Especially, the peak pressure of the shock wave is captured.

1. Introduction

With the development and improvement of the underwater guidance technology, the probability of ships subjected to the near-field underwater explosion rises rapidly, which contributes to much more attention received in the quantification of the wall pressure loading and structure protection subjected to the near-field underwater explosion. The loading generated by the near-field underwater explosion acting on the hull is extremely high and can cause serious damage to the structure of the ship and great casualties [1, 2]. The accurate assessment of the wall pressure loading generated by the near-field underwater explosion is an extremely important basis to design ship structures of high quality and save lives in conflicts or sea wars. Also, the accurate pressure loading information is of great help to some other interesting problems, such as the ice breaking [3].

Underwater explosion is an extremely complex procedure [4]. Immediately after the explosive charge is detonated, a strong shock wave will appear, and massive product gas is released, forming a high-pressure gas bubble in the water. The shock wave propagates in the water at a very high speed. When the shock wave gets at a structure, a high-pressure loading will act at the surface of the structure [5]. Here, the pressure loading due to the shock wave is called as shock wave loading (SWL). The pressure inside the gas

bubble is much higher than that of the surrounding water after the detonation. As a result, the bubble will expand fast. With the expansion of the bubble, the pressure inside the bubble decreases and the pressure of the surrounding water increases. Due to the inertia, the bubble will continuously expand when the pressure inside the bubble is equal to that of the surrounding water [6]. The overexpansion leads to the pressure inside the bubble to become lower than that of the surrounding water. Then, the bubble stops expanding and begins to collapse. In the case that the charge is detonated near the surface of a structure, a high-speed water jet will develop with the help of the Bjerknes effect, the inertia and the influence of gravity [7]. This water jet will traverse the whole bubble at a very high velocity and impact on the surface of the structure, acting another pressure loading on the surface [8, 9]. As the bubble continuously shrinks, it will reach its minimum volume, releasing a high-pressure wave [3]. Then, the bubble will rebound its second cycle. Here, the pressure loading due to the jet and the bubble collapse is called as bubble-jet loading (B-J loading). So, the pressure loading, generated by a near-field underwater explosion, on the surface consists of a shock wave loading and a series of continuous bubble-jet loadings [10].

The experiment is a direct way to obtain and investigate the pressure loading generated by an underwater explosion. During World War Two, to meet with the military needs, many experiments focusing on the basic explosive properties, the peak pressure of the explosion shock wave, the bubble pulses, the bubble periods, and the bubble behaviour near boundaries, were carried out. After the war, Cole [11] collected these experiment results and published them in the Underwater Explosions in which much useful data and simple theoretical modelling of the underwater explosion loading are included. Because of some key reasons such as the high cost and safety concerns, the real-scale underwater explosion experiment becomes very rare [12]. Brett et al. [13] conducted a series of small-scale experiments to investigate the response of a cylindrical steel target instrumented with accelerometers and underwater pressure transducers subjected to near-field underwater explosions generated by plastic explosive PE4 with two charge sizes of 5 g and 10 g. The underwater pressure transducers were PCB 138A05 type with a 35 MPa maximum capability. The free-field water pressure loading was recorded and studied. Klaseboer et al. [5] used three pressure transducers to get the pressure profiles of the free-field pressure loading to investigate the dynamics of underwater explosion bubble, generated by explosive Hexocire. Hung et al. [14, 15] conducted some experiments to investigate the underwater explosion bubble near different boundaries using only detonator as the explosion source. A PCB 138A pressure transducer was used to record the free-field pressure. Krieger and Chahine [16] investigated the acoustic signals, which were recorded by PCB Piezotronics model 102A03 pressure transducer, generated by underwater explosion near surface. The spark was used as the underwater explosive source. Fan et al. [17] developed a new underwater pressure transducer using polyvinylidene fluoride as the sensing element to record and investigate the free-field pressure loading. The literatures mentioned above focus on the assessment and investigation of the free-field pressure loading of the underwater explosion, as well as Li et al. [18] using a high-voltage spark as the explosion source. Compared with the assessment of the free-field pressure loading by experiment, the measurement of the wall pressure loading generated by near-field underwater explosion is much rarer. In the experiments conducted by Lee et al. [19] to investigate the deformation and rupture of the thin steel plates subjected to close-proximity underwater explosion, a pressure transducer was located directly on the surface of the target plate to record the pressure loading acting on the surface of the plate. However, it must be pointed out that the pressure loading in the water near the surface was recorded actually. Jayaprakash et al. [20] conducted a series of experiments to investigate the interaction between a spark-generated bubble and a vertical wall on which a PCB-101A03 pressure transducer was flush mounted. The wall pressure loading due to the bubble collapse was recorded, and the two peaks of the pressure signals were studied. Cui et al. [12] conducted a series of small-charge underwater experiments to study the bubble dynamics near various boundary conditions. In their experiments, pressure transducers were placed in the water and on the target plate to record both free-field and wall pressure loading. And the wall pressure loading was studied in detail. Also, some other researchers, such as Li et al. [21, 22], Wang et al. [23], and Klaseboer et al. [24] studied the pressure due to the bubble by numerical methods. From the literatures mentioned above, the assessments of free-field and wall pressure loading have attracted many researchers. However, the experiments aiming at the measurement of the wall pressure loading are rarer than those aiming at the measurement of free-field pressure loading.

In this article, a new lab-scale experimental system is developed and manufactured to assess the wall pressure loading, generated by a near-field underwater explosion, on the surface consisting of a shock wave loading and a series of continuous bubble-jet loadings. In this system, a Hopkinson [25] or Kolsky [26] pressure bar (HPB), which is inserted through the hole is drilled through the center of the circular target plate. And the face of the HPB end lies flush with the loaded face of the target plate. Here, the HPB is used as the sensing element to record the pressure loading acting on the HPB end face. This methodology has been used by Leiste [27] and Rigby et al. [28–32] to measure the pressure loading subjected to the explosives buried in ground, by Cloete and Nurick [33] to measure the pressure loading of blasts in the air, and by Park et al. [34] to assess the pressure loading subjected to sand column impact. However, it must be pointed out that only one phase pressure loading is recorded by this methodology in these literatures, and there is no restraint on the axial motion of the HPB. As a result, the end face of HPB may not flush with the loaded face of the target plate after one phase pressure loading, which means it is no longer suitable for assessing the bubble-jet loading. As mentioned above, the whole pressure loading on the surface generated by a near-field underwater explosion consists of a shock wave loading and a series of continuous bubble-jet loadings. Some improvements must be made on this methodology before this

methodology can be used to measure the wall pressure loading subjected to a near-field underwater explosion. Firstly, the whole apparatus must be suitable for the underwater environment. A waterproof tube, on which the target plate is mounted, is added to enclose the HPB and the strain gauges mounted on the HPB. The waterproof tube is fixed on the supported frame. Secondly, the HPB must be ensured flush with the loaded face of the target plate to assess the B-J loadings. A hard rubber cylinder is placed at the distal end, and a pair of ropes taped on the HPB is used to pull the HPB against the rubber cylinder tightly so that the end face of the HPB is ensured flush with the loaded face of the target plate. With the help of these two improvements, this methodology can be used to assess the wall pressure loading generated by a near-field underwater explosion.

It must be pointed out that assessing the wall pressure generated by a close field underwater explosion by using the established measurement technique given above is relatively new. Before it can be used to measure the underwater explosion wall pressure, the question weather the pressure obtained from the stress wave information equals to the real wall pressure must be answered. To validate the pressure measurement technique based on the HPB, a series of underwater explosion between two parallelly mounted circular target plate experiments are conducted. Firstly, experiments are conducted to validate the assumption that pressure profiles at the two points on the two plates which are symmetrical to each other about the middle plane of symmetry are the same. After the assumption is proved correct, the validating experiments of the measurement technique based on HPB are carried out.

In this article, a series of the minicharge underwater explosion experiments are conducted in a water tank to validate and investigate the capability of the improved methodology and experiment system to assess the wall pressure loading generated by a near-field underwater explosion. A minicharge is chosen as the explosion source to meet the safe requirement of the lab. Some semiconductor strain gauges are mounted on the HPB to record the axial strain. The strain data are recorded by a National Instruments (NI) PCIe-6376 data acquisition unit (DAU). Also, a high-speed video (HSV) camera is used to capture the images of each underwater explosion experiment, which are used to study the wall pressure loading coupled with the strain data. The camera and the DAU are triggered synchronously. The results of experiments are presented in detail and analyzed carefully. According to the assessed wall pressure loading and the associated images, the proposed methodology and experiment system can be used to capture the shock wave loading and bubble-jet loadings.

The rest of this article is arranged as follows. In Section 2, the experimental work, in which the experimental apparatus and the test plan are included, is given in detail. The results of the experiments and the analysis are presented in Section 3. In Section 4, some concluding remarks and recommendations for the future work are presented.

2. Experimental Work

In this section, the details about the test apparatus and the whole test system are given. The test plane which is conducted in this paper is also given. It should be pointed out that the apparatus and the test system are designed to meet the requirements of the lab-scale experiment. If this methodology is to be used to conduct the large-scale experiments, the apparatus and the whole test system should be redesigned and manufactured carefully. But the kernel of this methodology is same.

2.1. Apparatus and Test System. All the experiments conducted in this article are carried out on a strong enough aluminium alloy frame, as shown in Figure 1. The water tank with a dimension 600 mm × 600 mm × 600 mm, where the underwater explosion occurs, is made up of high transparent reinforced glass with a thickness of 12 mm. The good transparency of the glass allows capturing the bubble dynamics by the HSV camera with the help of the light provided by the halogen light. All the experiments conducted in this article are captured at a resolution of 384 × 384 with a rate of 40000 fps and 14 μs exposure time. A minicharge of powder of fire cracker is used as the explosive source, which is detonated by a spark generator. The powder of fire cracker consists of 55% ~ 65% of potassium perchlorate powder, 18% ~ 23% of aluminium powder, 10% ~ 15% of ferrotitanium powder, and about 5% of manganese dioxide powder. As mentioned above, the discharge of a high-voltage charge stored in capacitors can generate a considerable underwater explosion bubble which may have an influence on the underwater explosion generated by the minicharge. To minimize the influence of the underwater explosion bubble due to the spark, a low-voltage spark generator should be used. Here, a 50 V charger stored in a 50 μF capacitor is used as the detonator, the maximum diameter of the underwater explosion bubble generated by which is less than 2 mm. When the charge is detonated, the capacitor will apply a voltage, high-current pulse on the wire in the charge. This rise edge signal is a perfect signal to trigger the oscilloscope and the HSV camera. The explosive charge is positioned by a 3D fixator to the expected position.

A 12 mm thick, 250 mm diameter stainless steel plate serves as the target plate, which is big enough to conduct the near-field underwater explosion. To meet the requirement of the underwater condition, the target plate is mounted on the end of a waterproof tube, as shown in Figure 2. Of course, some seal rings are used.

The elastic stress wave due to the wall pressure loading propagates in the HPB. When it reaches the distal end of the HPB, it will return. The strain gauge will record a superposition signal of the still-incoming stress wave and the reflected wave from the distal end. In our experiments, the bar is chosen to be 2.3 m long. And the strain gauges are placed 0.1 m from the loaded face of the HPB. As a result, there will be about 0.9 ms before the arrival of the reflected wave from the distal end. Violent underwater explosions cannot be conducted in the lab, which means the wall pressure loading acting on the loaded face of the HPB is very small. To get an intensive enough signal which can be detected and a higher signal-to-noise ratio (SNR), some special design and treatments are adopted here. Firstly, the

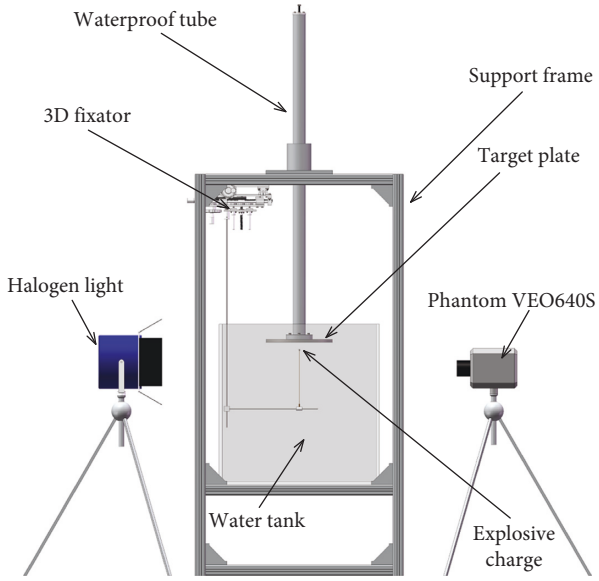

Figure 1: Schematic of the test system.

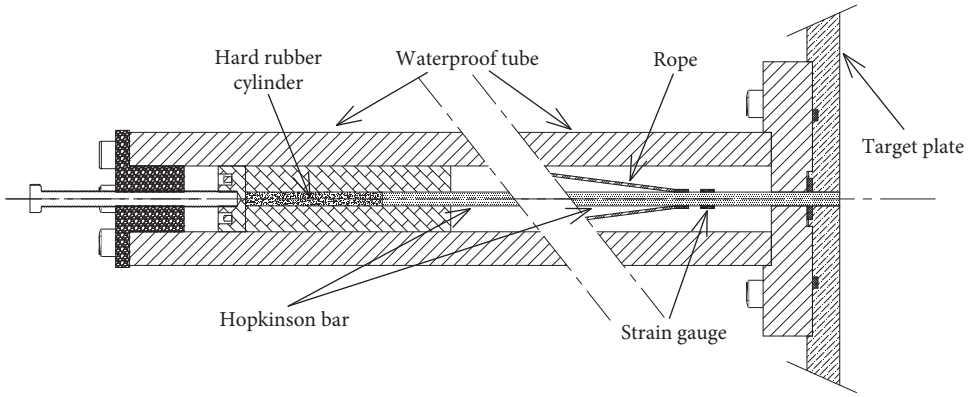

Figure 2: Detailed schematic of the apparatus.

aluminium alloy bar is chosen as the HPB. The elastic modulus of the aluminium alloy is smaller than that of copper and steel, which means a higher strain signal can be obtained under the same pressure loading when an aluminium bar is used. Secondly, semiconductor strain gauges, which are more sensitive than wire gauges, are adopted to detect the weak strain signal. Besides, the gauges are mounted on the perimeter of the HPB in pairs, and a Wheatstone bridge circuit is used as the gauge input configuration to detect the axial strain component only. As mentioned above, the wall pressure loading consists of a shock wave loading and a series of continuous bubble-jet loadings. To make sure the loaded face of the HPB flushes with the loaded face of the target plate after the action of the shock wave loading, the HPB is pulled by a pair of ropes, taped on the HPB, against a hard rubber cylinder, which is located in a tube and mounted to the waterproof tube through an adjusting screw, hard, as shown in Figure 2.

As mentioned above, before this measurement technique can be used to measure the underwater explosion wall pressure, the question weather the pressure obtained from the stress wave information equals to the real wall pressure must be answered by experiments. Immediately after the explosive is detonated, the shock wave propagates in the formation of spherical wave, which means at any point on the spherical wave front, the shape of the shock wave pressure profile should be the same. When an explosive charge located on the middle plane of symmetry of two parallel plates is detonated, the shock wave pressure profiles at the two points on the two plates which are symmetrical to each other about the middle plane of symmetry should be the same. On one of the two points, the measurement technique based on the HPB is used to get the pressure of this point. And on the other point, a pressure transducer is used to get the pressure of the other points. By comparing the two obtained pressure profiles, the measurement technique based on the HPB can be validated. However, it must be pointed out the assumption that the two pressure profiles of the two points are the same is based on the theoretical analysis. So, the experiments to examine whether the two pressure profiles are the same are set up firstly by using two pressure transducers to get the two pressure profiles at these two points.

As same as in the test system in Figure 1, the target plates are circular stainless plates with a thickness of 12 mm and a diameter of 250 mm. The two target plates are mounted together coaxially and parallelly through four adjusting columns, as shown in Figures 3 and 4. Each adjusting column has a length of 30 mm, which means the gap between the two target plates is 60 mm, and the distance between the explosive charge and each target plate is 30 mm.

The pressure transducers used for this validating experiments are the piezoelectricity type pressure transducers of Sinocera Piezotronics, Inc., (http://www.china-yec.com) together with a YE5853 low-noise charge amplifier. The pressure transducers' model names are CY-YD-205. The used pressure transducers have a maximum measurement pressure of 30 MPa.

2.2. Test Plane. To validate and investigate the capability of the improved methodology and experiment system to assess the wall pressure loading, a series of underwater explosion experiments are conducted. The explosion source used in the experiments is a charge of 0.110 ± 0.001 g explosive, the maximum radius of the underwater explosion bubble generated by which is 70.0 mm in free-field conditions according to the results of the experiments presented in the next section. The experiments to examine whether the two pressure profiles on the two parallelly mounted target plates are conducted firstly. Then, the experiments to validate the established measurement technique based on Hopkinson bar are carried out. Finally, a series of close field underwater explosion experiments with different stand-off distances are carried out to investigate the capability of the established measure technique to assess the wall pressure loading. The stand-off distances of the experiments are chosen as 5, 10, 15, ..., 35 mm. The experiments conducted in this article are summarized in Table 1.

3. Results and Discussion

3.1. Underwater Explosion in a Free Field. Firstly, the underwater explosion in a free field is conducted. The depth of the water in the tank is 550 mm. The charge is located at a depth of 380 mm from the bottom. The images in Figure 5 show the first cycle of the underwater explosion bubble generated by the explosive charge of 0.11 g. From these images, the bubble expands quickly after it is detonated and gets to its maximum volume at 6.6429 ms after the detonation. The maximum radius of the bubble is about 70 mm which is obtained from images by pixels. 12.5 microseconds after the detonation, the first collapse of the bubble occurs, which means the first bubble period is 12.5 ms.

3.2. Validating Experiments. As mentioned above, before the measure technique based on Hopkinson bar to assess the wall pressure loading, the question that whether the pressure loading obtained based on the shock stress wave is equal to the real wall pressure loading due to the near-field underwater explosion must be answered.

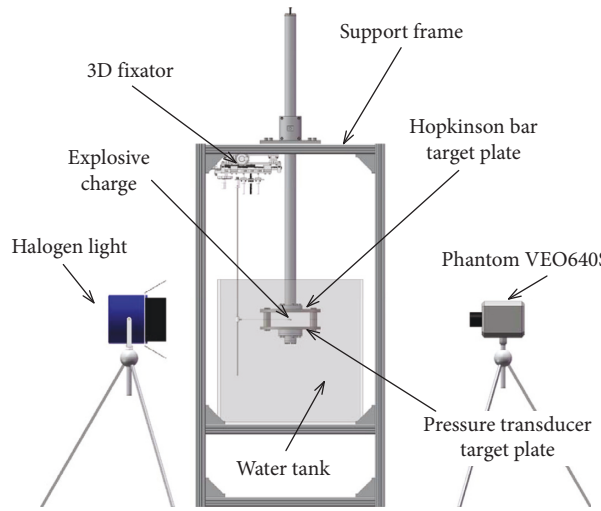

Figure 3: Schematic of the test system of validity.

Here, the underwater explosion between two coaxially and parallelly mounted circular target plates is planned to be used as the validating system. First of all, the assumption that the shock wave pressure profiles at the two points on the two plates which are symmetrical to each other about the middle plane of symmetry are the same should be proved to be correct by experiments.

About 1.71 ms after the high-current pulse is applied, the explosive charge is detonated, and the underwater explosion begins as shown in Figure 6(b). Due to the special boundary of two parallel plates, the underwater explosion bubble does not extend to a sphere but a ellipsoid as shown in Figure 6. Immediately when the explosive charge is detonated, the shock wave appears and propagates in the water. When the shock wave arrives at the upper and lower target plates, the pressure-loading can be obtained by the pressure transducers as shown in Figure 7. According to the pressure-time profiles of the upper and lower target plates shown in Figure 7, the pressure-time profiles of the upper and lower plates coincide with each other. The same conclusion can be also obtained in the other two same experiments as shown in Figure 8.

The relative errors between the upper and lower target plates' peak pressure are given in Table 2. The relative errors are less than 2.0%. From the results, the assumption that the shock wave pressure profiles on the two points on the two plates which are symmetrical to each other about the middle plane of symmetry are the same is correct can be obtained. Further, this system can be used to validate the capacity of the pressure measure technique based on the HPB.

By replacing the pressure transducer fixed on the upper target plate by the Hopkinson bar, the system is used to validate the capacity of the pressure measurement based on the HPB. The pressure profiles obtained by the HPB and the pressure transducer are shown in Figure 9. From Figure 9, the profile obtained by the HPB coincides well with the profile obtained by pressure transducer before the reflected stress wave arrives at the point where the strain gauges are fixed. Other two same experiments are also conducted to validate the measurements further. The profiles are given in

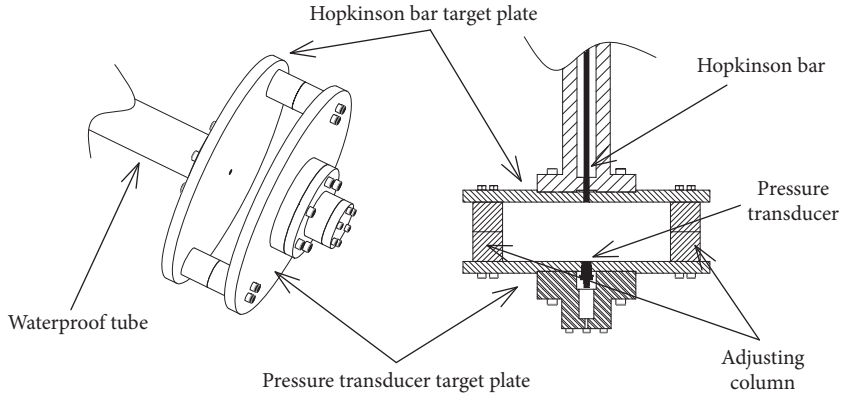

Figure 4: Detailed schematic of the apparatus of the validity system.

Table 1: Tests plane.

Tests	Charge (g)	Boundary condition	Stand-off (mm)
1–3	0.110	Free-field	–
4–6	0.110	Between two plates with two pressure transducers	–
7–9	0.110	Between two plates with Hopkinson bar and one transducer	–
10	0.110	Below the target plate	5
11	0.110	Below the target plate	10
12	0.110	Below the target plate	15
13	0.110	Below the target plate	20
14	0.110	Below the target plate	25
15	0.110	Below the target plate	30
16	0.110	Below the target plate	35

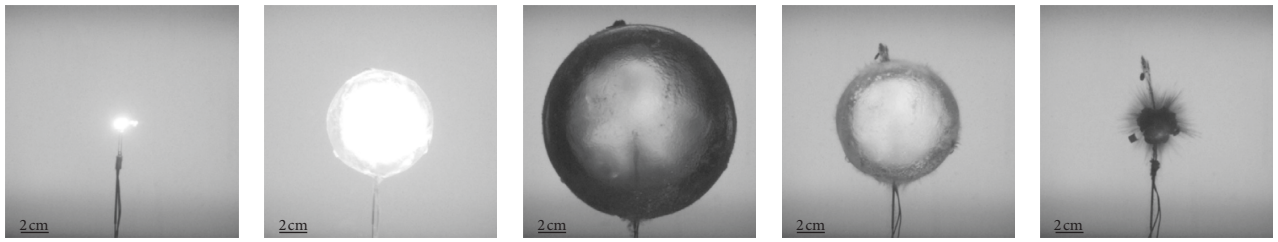

Figure 5: Evolution of the first cycle of the underwater explosion bubble's expansion and collapse in a free field generated by the explosive charge of 0.11 g. (a) $t = 0.0000$ ms. (b) $t = 1.0000$ ms. (c) $t = 6.6429$ ms. (d) $t = 11.0000$ ms. (e) $t = 12.5000$ ms.

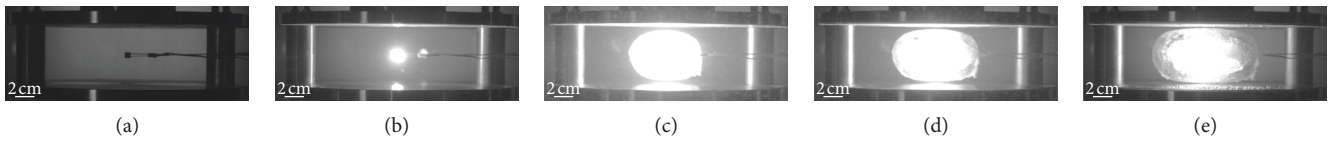

Figure 6: Evolution of the underwater explosion bubble's expansion between the two coaxially and parallelly mounted plates by the explosive charge of 0.11 g. (a) $t = 0.0000$ ms. (b) $t = 1.7124$ ms. (c) $t = 2.9324$ ms. (d) $t = 3.5724$ ms. (e) $t = 4.5524$ ms

Figure 10 from which the same conclusion can be obtained. The peak pressure of these profiles and the relative errors are given in Table 3. It can be obtained that the relative errors between the peak pressures obtained by the Hopkinson bar and the pressure transducer are less than 2.0%. So, it can be reasonably deducted that the pressure loading obtained based on the shock stress wave is equal to the real wall pressure loading due to the near-field underwater explosion which is the key point of this measurement technique.

3.3. Experiment Results with 5 mm Stand-Off. Next, the system proposed and manufactured by us is used to measure the pressure loading on the target plate subjected to an

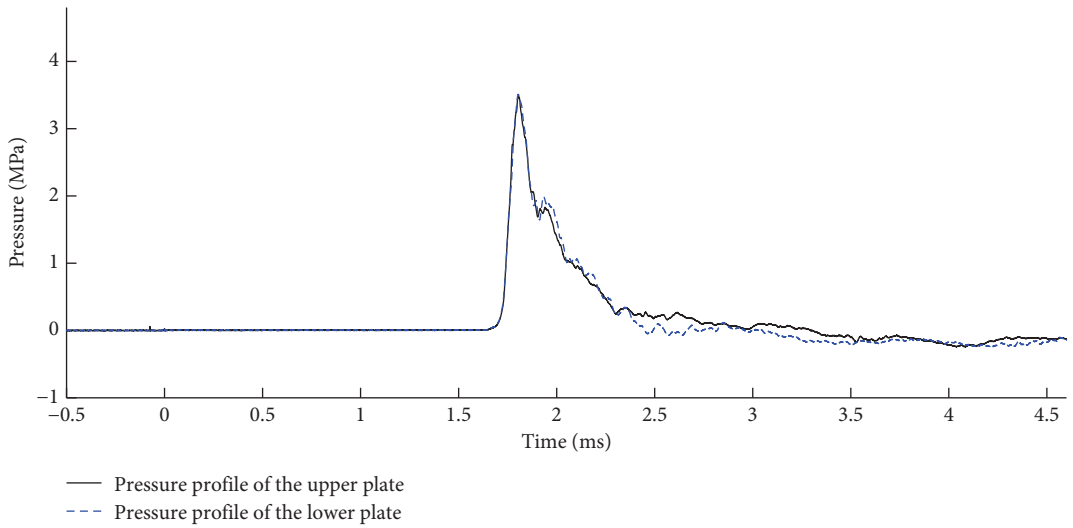

Figure 7: The comparison between pressure-time profiles of the upper and lower target plates.

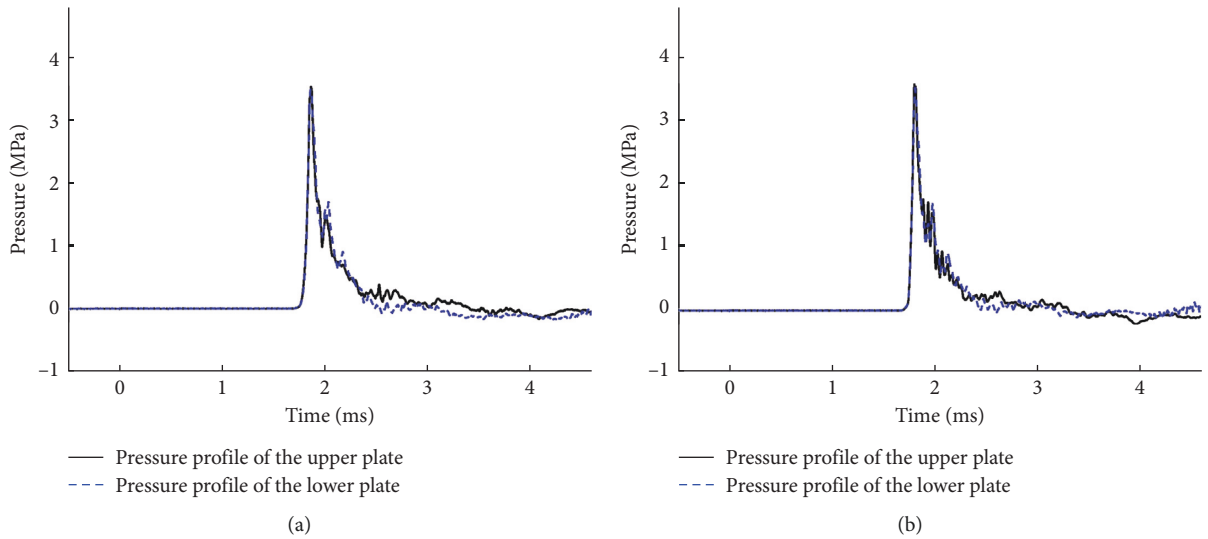

Figure 8: Pressure-time profiles of the upper and lower target plates of the other two experiments.

Table 2: The relative errors between the upper and lower target plates' peak pressure of these three experiments.

	Experiment 1	Experiment 2	Experiment 3
Upper target plate (MPa)	3.473	3.521	3.593
Lower target plate (MPa)	3.508	3.475	3.534
Relative error (%)	1.0	1.3	1.6

underwater explosion at 5 mm stand-off firstly. Figure 11 shows the pressure-time profile, and the evolution of the underwater bubble within the first two cycles of expansion and collapse is shown in Figure 12. Some important notes are added in Figure 11 to help analyze and study the pressure loading coupled with the frames of the underwater bubble in Figure 12.

The low-voltage spark generator begins to apply the voltage and high-current pulse on the wire in the charge at $t = 0.0000$ ms. The DAU and the HSV camera are triggered by this rising voltage signal. From the pressure-time profile in Figure 11, this detonation signal also leaves a noise on the pressure signal. After 1.72 ms, the explosive charge is detonated, and the underwater explosion begins as shown in Figure 12(b). Meanwhile, the shock wave is released into the water and acting on the target plate. From the pressure-time profile, the shock wave pressure loading on the target plate was precisely captured by the HPB-based pressure-loading measure system. The shock pressure loading rises rapidly to its peak pressure of 10.00 MPa and then decays down to 0.00 MPa. The stress wave due to the shock wave loading will propagate along the HPB and return when it reaches the distal end of the HPB. Then, it will reach the loaded end and return again and repeats over and over. The strain gauges placed on the HPB will record the initial stress wave due to the shock pressure loading one time and the reflected stress wave several times, just as shown in Figure 11. In Table 4, the

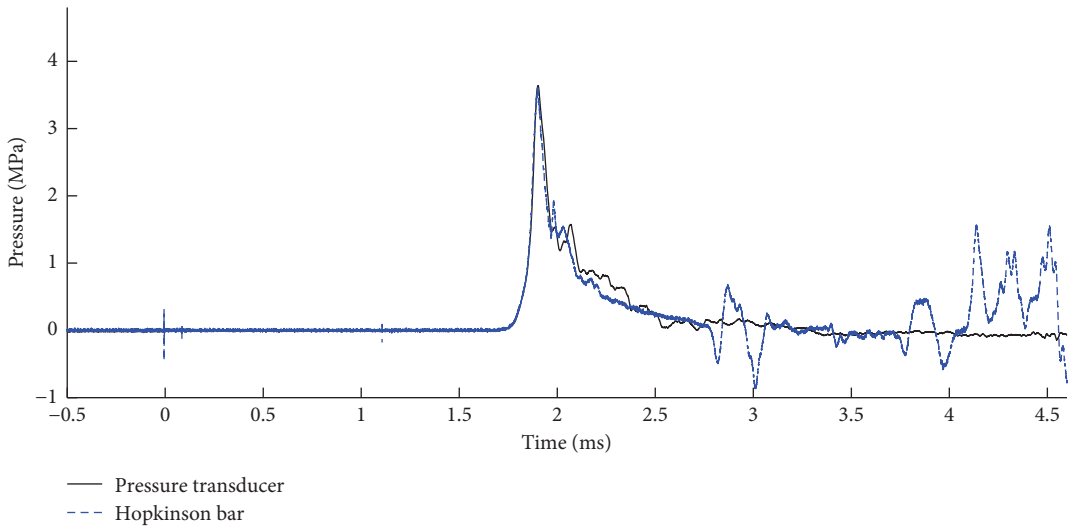

Figure 9: The comparison between pressure-time profiles obtained by Hopkinson bar and pressure transducer.

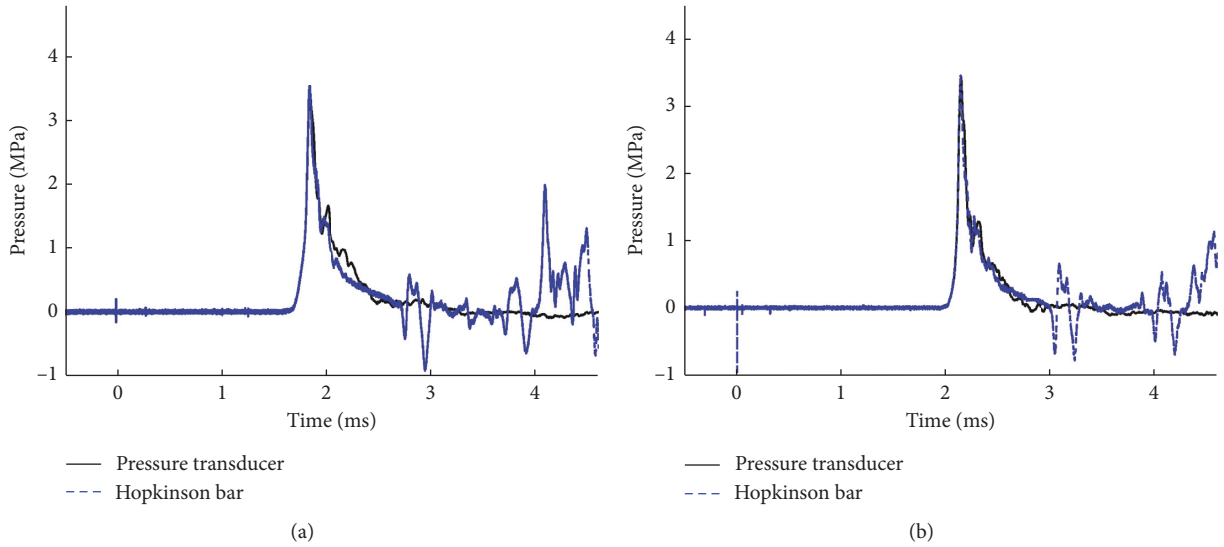

Figure 10: Pressure-time profiles obtained by Hopkinson bar and pressure transducer of the other two experiments.

Table 3: The relative errors between peak pressure obtained by the Hopkinson bar and the pressure transducer of these three same experiments.

	Experiment 1	Experiment 2	Experiment 3
Hopkinson bar (MPa)	3.605	3.545	3.455
Pressure transducer (MPa)	3.638	3.485	3.434
Relative error (%)	0.9	1.7	0.6

arrived times of the peaks of initial wave and reflected wave are given, and the delay times between these peaks are calculated. According to the delay time, the stress wave travels over the twice the length of the HPB in 0.934 ms. So, the velocity of the stress wave propagation in the HPB is 4.9 km/s. After several reflections, the peak of the reflected stress wave decays quickly to a very low level, which is enough for the detection of the following pressure loading due to the bubble.

Massive gas is released after the charge is detonated and forms an underwater bubble, as shown in Figure 12(c). The bubble expands rapidly to its maximum volume 8.7245 ms after the rising voltage signal is implied. Figure 12(d) shows the shape of the biggest bubble. Then, the bubble begins to shrink. Due to the Bjerknes effect, the bubble is attracted towards the target plate, as shown in Figure 12(e), and a water jet develops from the distal side of the bubble. This water jet will travel through the whole bubble and impact on the target plate. Then, the bubble shrinks to its minimum volume 16.23 ms after the detonated signal as shown in Figure 12(f). In the meantime, the pressure loading due to the bubble will reach its peak pressure of 9.64 MPa, as shown in the pressure-time profile in Figure 11. As with the stress wave due to the shock wave loading, the stress wave due to the bubble will return at the ends of the HPB. There are also several reflected waves of the stress wave due to the bubble. After the bubble reaches its first minimum volume, it will

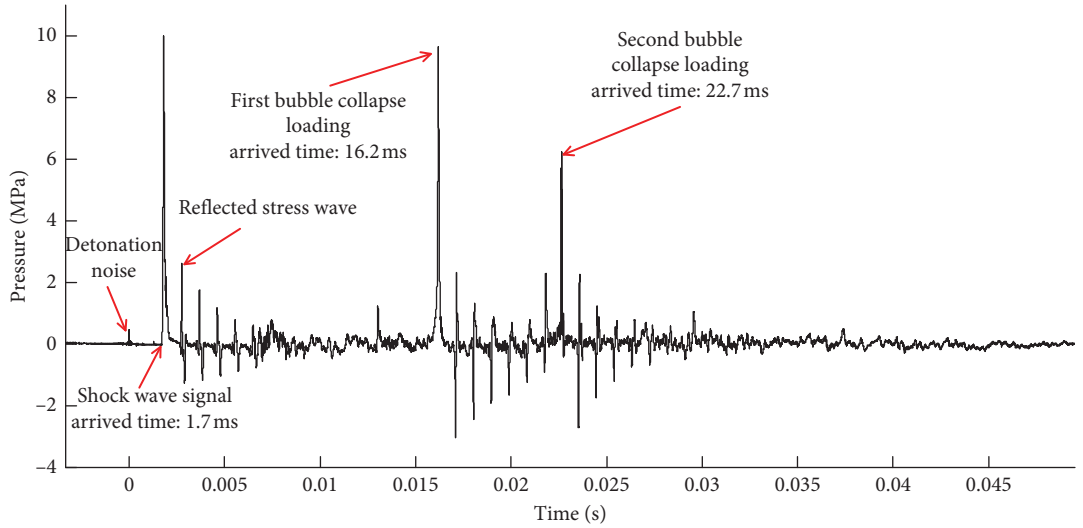

Figure 11: Pressure-time profile recorded by HPB with a 5 mm stand-off.

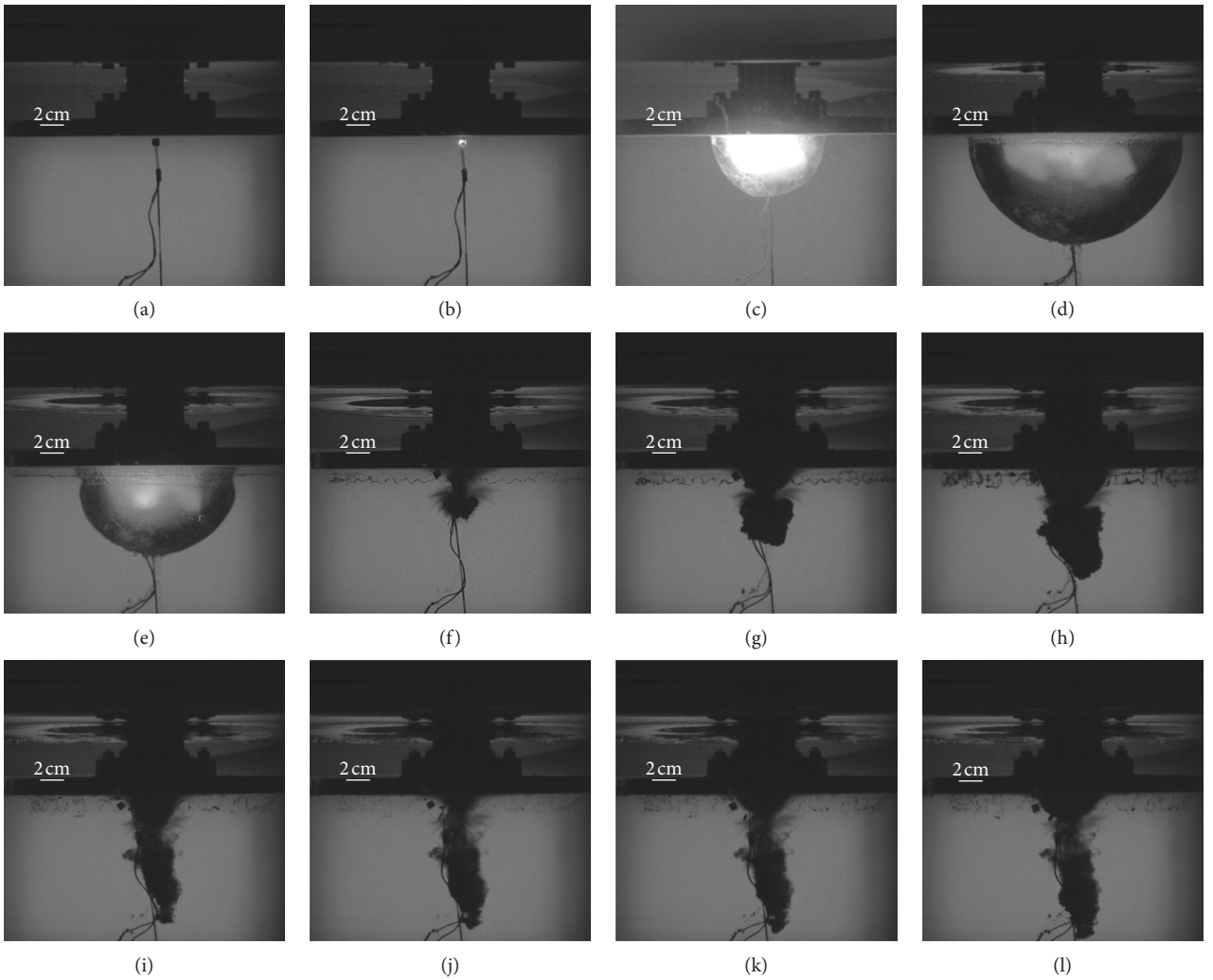

Figure 12: Evolution of the first two cycles of the underwater explosion bubble's expansion and collapse below the target plate with 5 mm stand-off. (a) $t = 0.0000$ ms. (b) $t = 1.7245$ ms. (c) $t = 6.6245$ ms. (d) $t = 8.7245$ ms. (e) $t = 13.4495$ ms. (f) $t = 16.2295$ ms. (g) $t = 17.2745$ ms. (h) $t = 19.4495$ ms. (i) $t = 21.9745$ ms. (j) $t = 26.6995$ ms. (k) $t = 23.2745$ ms. (l) $t = 24.4745$ ms.

Table 4: The delay time between the peaks of initial wave and reflected waves.

	Initial wave	First reflected wave	Second reflected wave	Third reflected wave	Forth reflected wave
Arrived time of peak (ms)	0.001815	0.002749	0.003683	0.004617	0.005551
Delay time from previous peak (ms)	–	0.934	0.934	0.934	0.934

expand again, beginning its second cycle of expansion and collapse, as shown in Figures 12(g)–12(i). A second bubble collapse loading is detected when the bubble reaches its minimum volume for the second time, as shown in Figure 12(j). The bubble will continue the cycles of expansion and collapse. As the bubble expands and collapses, the energy of the bubble is dissipated and released. After the first two cycles, the energy of the bubble becomes very low, which means the pressure loading due to the corresponding bubble collapse is so low that it cannot be detected, as shown in the pressure-time profile. According to the reflected stress wave of the shock wave loading, it can clearly be concluded that the reflected stress wave decays quickly to a very low level. This phenomenon also appears in the reflected stress wave pulses within the portion of the stress wave history due to the underwater explosion bubble. For the stress wave due to the first bubble collapse, the first five reflected stress wave signals decay rapidly. For the stress wave due to the second bubble collapse, the reflected stress wave decays rapidly. However, the sixth reflected stress wave's amplitude is larger than the fifth reflected stress wave's amplitude abnormally. The reason why this abnormal phenomenon occurs is unknown for the present. It cannot be concealed that the present measurement technique and methodology are not perfect, and there are many issues of this measurement methodology to study. However, the bright point that the proposed methodology can be used to measure the pressure loading generated by an underwater explosion cannot be darkened.

From the results of the experiment of underwater explosion under the target plate at 5 mm stand-off distance, the pressure measure system proposed and manufactured by us can detect and record the pressure loading due to the shock wave and the first two bubble collapse preciously. The signal obtained by the proposed method is a superposition of the stress wave due to the pressure loading and the reflected stress wave. In practice, to obtain the real pressure loading, the first thing is to obtain the duration it takes the stress to travel the twice the length of the HPB. Then, according to the high-speed video of the underwater explosion or the signal obtained by the HPB, the start time of the shock wave loading or the pressure loading due to the bubble can be obtained. The start time of the signal superposition can be determined by moving the start time of the pressure loading back by the duration. The real pressure signal located in the gap between the start time of the pressure loading and the start time of the signal superposition is the pressure signal which is wanted. Next, the other experiments with different stand-off distances are conducted to investigate our experimental system further.

3.4. Experiment Results with $10-35$ *mm Stand-Off.* In Figures 13 and 14, the pressure loadings due to the underwater explosion below the target plate at 10 mm, 15 mm, ..., 35 mm stand-off distances recorded by the HPB are shown. From the pressure-time profiles, the pressure measure system can capture the pressure loading due to the shock wave at 10 mm, 15 mm, ..., 30 mm stand-off distances. The first reflected stress wave arrives after the end of the stress wave due to the shock wave, which means the length of the HPB is long enough to record the whole pressure loading due to the shock wave. However, as shown in Figure 14(c), the first reflected stress wave arrives before the end of the initial stress wave when the stand-off becomes 35 mm. This means that just part of the whole pressure loading due to shock wave is well recorded by the HPB. But the peak pressure of the shock wave loading is captured preciously, which is also of great help and significance for the engineer. The peak pressure loading-stand-off is given in Figure 15, from which it can be seen that the peak pressure loading decreases as the stand-off rises.

For the pressure loading due to the bubble, the pressure loading due to the first bubble's collapse is captured preciously at 10 mm, 15 mm, ..., 30 mm stand-off distances. As the stand-off rises, the duration of the pressure loading becomes long. This is due to that a considerable water jet due to the bubble shrinking develops and impacts on the target plate before the bubble's collapse. Here, we take the underwater explosion experiment at 25 mm stand-off as example to explain this. The evolution of the water jet and collapse of the underwater bubble at 25 mm stand-off is shown in Figure 16. Due to the Bjerknes effect, the bubble is attracted towards the target plate, and the velocity of the water near the distal side of the bubble becomes higher and higher, as shown in Figure 16(a), and water jet develops. After 15.6060 ms, the water jet travels through the whole bubble and impacts on the target plate, as shown in Figure 16(b). The pressure loading due to the bubble's jet begins to act on the target plate, which is detected by the HPB, as shown in the pressure-time profile in Figure 14(a). The bubble continues to shrink and reaches its minimum volume at $t = 16.0810$ ms, as shown in Figure 16(d). A shock wave is released when the bubble collapses, and this pressure loading is captured by the HPB, as shown in the pressure-time profile. Compared with the pressure loading due to water jet, the pressure loading due to bubble collapse has a higher peak pressure, but the duration is extremely shorter.

As the stand-off rises, the time between the beginning of the water jet impacting on the target plate and the bubble collapse also increases. So, the duration of the pressure loading due to the water jet and the bubble collapse becomes longer, which will go beyond the capability of the HPB. From the local enlarged pressure-time profile at 35 mm stand-off captured by HPB in Figure 17, the duration of the stress signal due to the jet and bubble collapse is more than

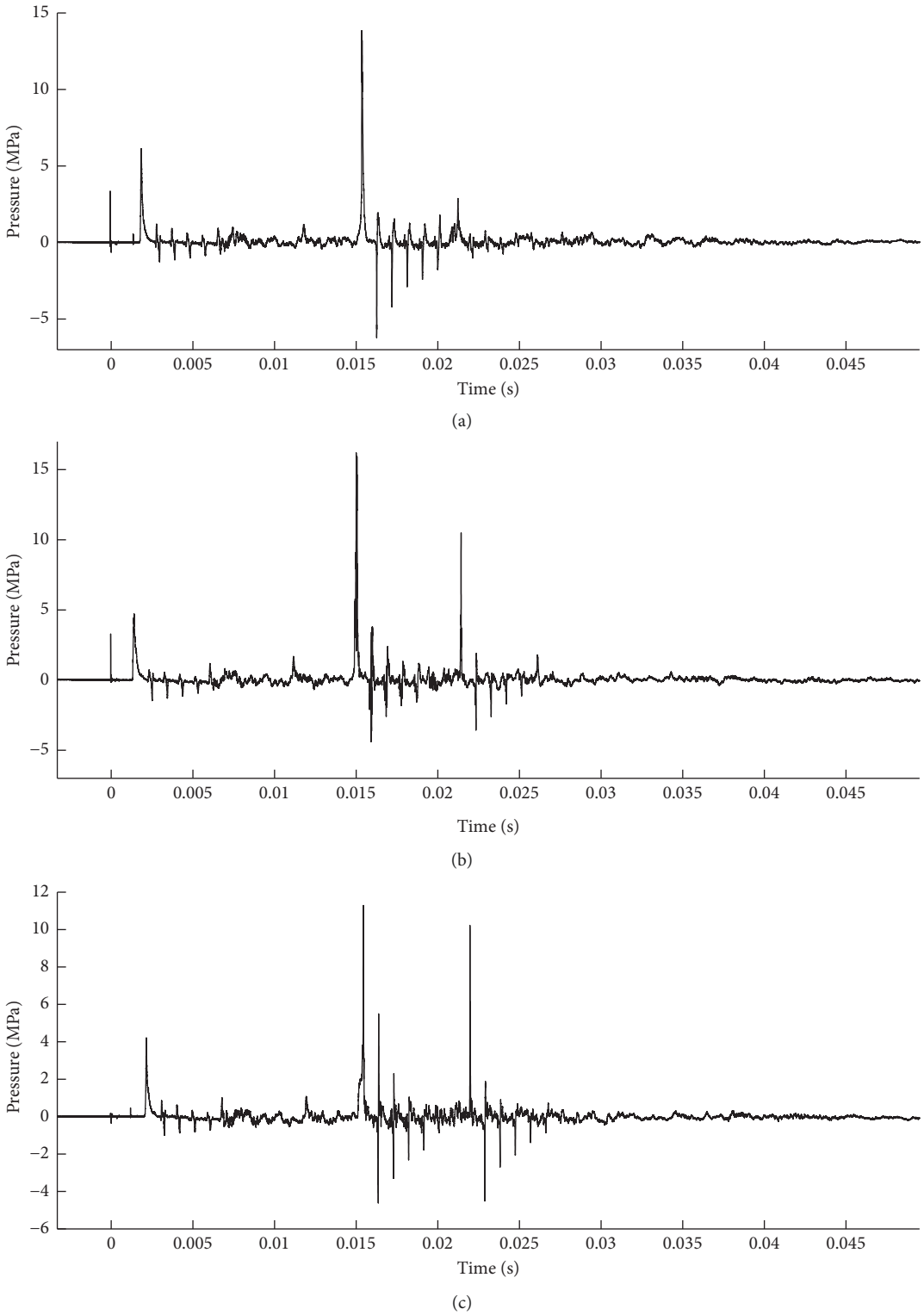

Figure 13: Pressure-time profile recorded by HPB with (a) 10 mm, (b) 15 mm, and (c) 20 mm stand-off.

1.24 ms during which the stress wave can propagate more than 6 m, which is much longer than the twice the length of the HPB. So, this stress wave signal is a superposition signal of the still coming stress wave and the reflected wave, which means the HPB can only capture part of the pressure loading due to the jet and bubble collapse at 35 mm stand-off distance.

According to the results and analysis given above, it can be seen that if the duration of the pressure loading is too much long, the reflected stress wave will go into the still

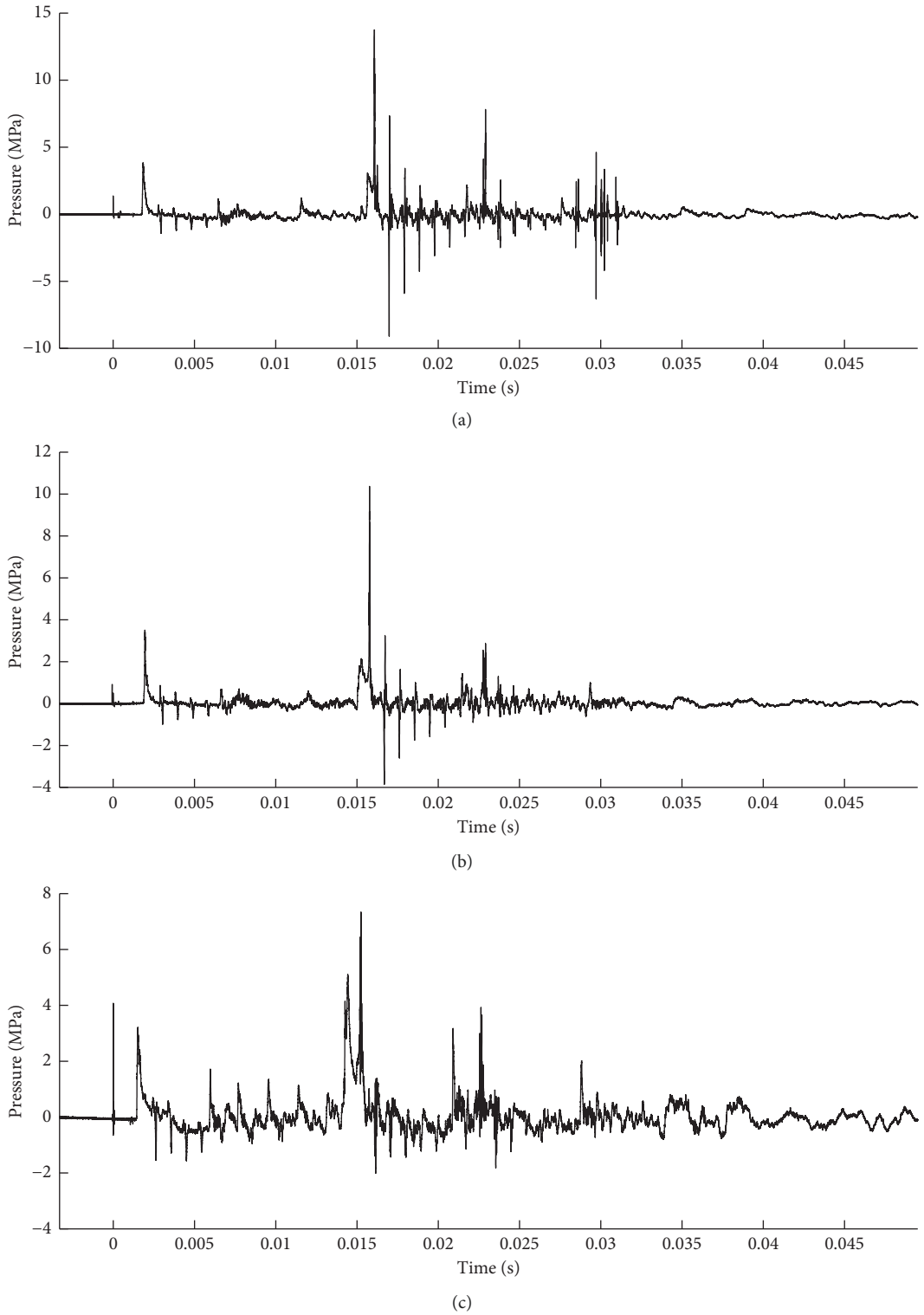

Figure 14: Pressure-time profile recorded by HPB with (a) 25 mm, (b) 30 mm, and (c) 35 mm stand-off.

coming stress. The obtained signal is a superposition of the reflected signal and the still coming signal which makes it difficult to recognize the real pressure loading. As mentioned above, the duration of the pressure loading due to the jet increases when the stand-off grows. The measurement technique based on the HPB is no longer suited for assessing this jet loading. In a word, the measurement technique based on the HPB can be only used to measure the loadings which have short durations. The loading of the near-field underwater explosion is a sort of this loading.

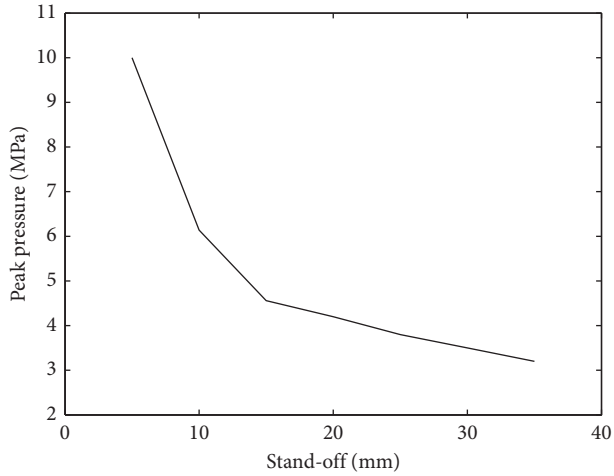

Figure 15: Peak pressure loading versus stand-off.

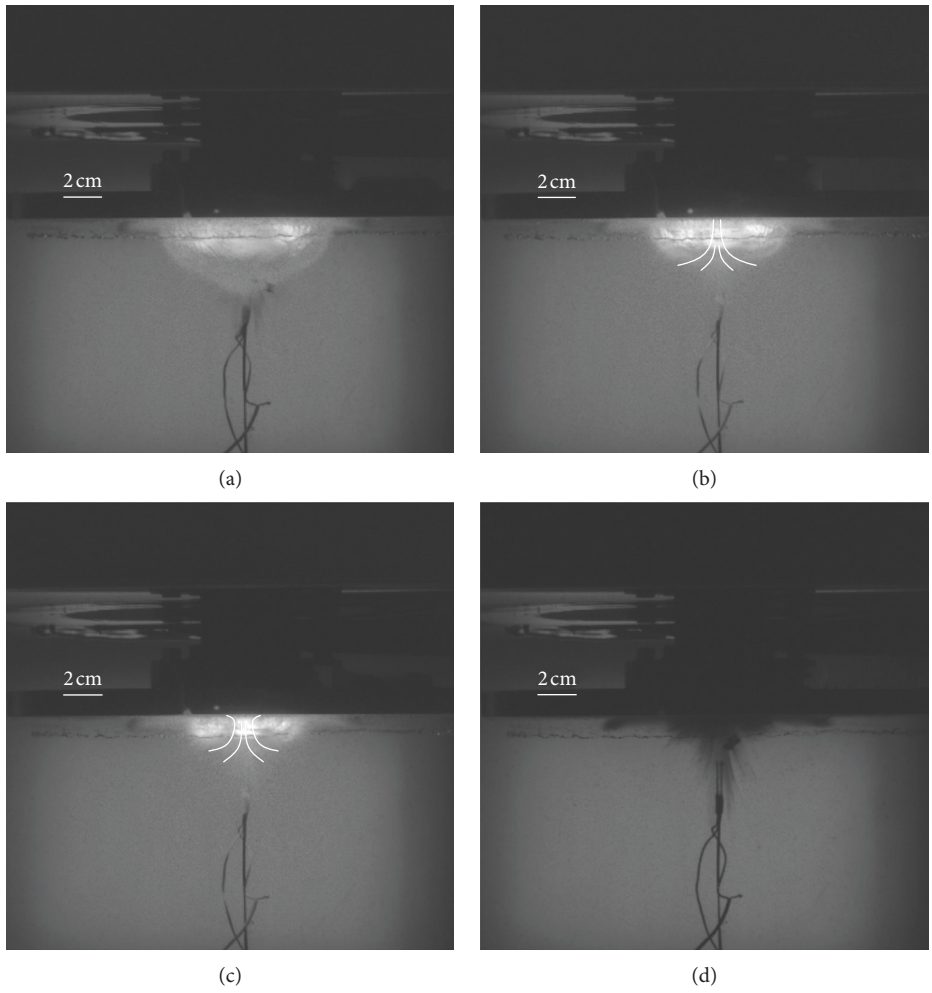

Figure 16: Evolution of the jet and collapse of the underwater bubble below the target plate with 25 mm stand-off. (a) $t = 15.2060$ ms. (b) $t = 15.6060$ ms. (c) $t = 15.8560$ ms. (d) $t = 16.0810$ ms.

4. Conclusions

In this article, a lab-scale experimental system is proposed and manufactured to measure the wall pressure loading generated by a nearby underwater explosion on the surface which consists of a shock wave loading and a series of continuous bubble-jet loadings. In this system, a Hopkinson bar, which is inserted through the hole drilled on the target

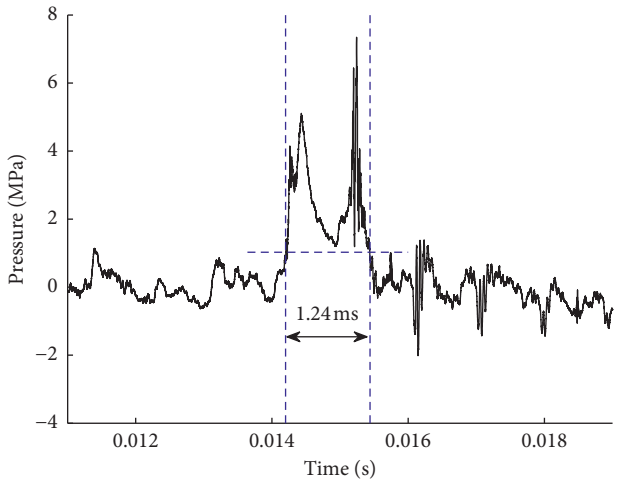

Figure 17: Local enlarged profile of the pressure-time profile at 35 mm stand-off in Figure 14(c).

plate, is used as the sensing element to detect and record the pressure loading. This methodology, which has been used to capture only one phase pressure loading in previous literatures, has been improved to make it be able to detect the underwater explosion pressure loading. Firstly, some waterproof units are added to make it suitable for the underwater environment. Secondly, a hard rubber cylinder is placed at the distal end, and a pair of ropes taped on the HPB is used to pull the HPB against the cylinder hard to make the HPB's end face flush with loaded face of the target plate during the bubble collapse. The pressure loadings are obtained according to the stress waves due to these pressure loadings which are recorded by the strain gauges tapped on the HPB. And a high-speed video camera is used to capture the evolution of the underwater explosion, which is used to analyze the wall pressure loading coupled with the recorded stress wave.

To validate the improved methodology and the experimental system, underwater explosions between two parallelly mounted circular target plates experiments are used as the validating experiments. Firstly, some experiments of this type are conducted to prove the assumption that that the shock wave pressure profiles at the two points on the two plates which are symmetrical to each other about the middle plane of symmetry are the same right. From the results, it can be said that the assumption is correct. Then based on this assumption, the key point of this methodology that the pressure got by the HPB is equal to the real pressure loading can be validated. According to the results of the following experiments of the same type, it can be reasonably concluded that the pressure loading obtained based on the shock stress wave is equal to the real wall pressure loading due to the near-field underwater explosion. To verify the capability of the improved methodology and experimental system, a series of minicharge underwater explosion experiments are conducted in a water tank. From the recorded pressure loading coupled with the images captured by the HSV camera, it can be seen that the improved methodology and experimental system can capture the pressure loading due to shock wave and the pressure loadings due to bubble-jet with 5 mm, 10 mm, . . ., 30 mm stand-off distances. When the stand-off distance becomes 35 mm, the durations of the shock wave pressure loading and bubble-jet pressure loading are so long that the experimental system can only capture part of the loading. However, these part loadings are of great help and significance for engineers, especially the peak pressure of the shock wave is captured preciously.

Conflicts of Interest

The authors declare that they have no conflicts of interest.

Acknowledgments

The authors would like to acknowledge the support of the Fundamental Research Funds for the Central Universities (HEUCFP201744) and the National Nature Science Foundation of China (51779056).

References

[1] F. Ming, A. Zhang, Y. Xue, and S. Wang, "Damage characteristics of ship structures subjected to shockwaves of underwater contact explosions," *Ocean Engineering*, vol. 117, pp. 359–382, 2016.

[2] Y. Liu, A. Zhang, Z. Tian, and S. Wang, "Numerical investigation on global responses of surface ship subjected to underwater explosion in waves," *Ocean Engineering*, vol. 161, pp. 277–290, 2018.

[3] P. Cui, A.-M. Zhang, S. Wang, and B. C. Khoo, "Ice breaking by a collapsing bubble," *Journal of Fluid Mechanics*, vol. 841, pp. 287–309, 2018.

[4] T. Li, S. Wang, S. Li, and A.-M. Zhang, "Numerical investigation of an underwater explosion bubble based on FVM and VOF," *Applied Ocean Research*, vol. 74, pp. 49–58, 2018.

[5] E. Klaseboer, K. C. Hung, C. Wang et al., "Experimental and numerical investigation of the dynamics of an underwater explosion bubble near a resilient rigid structure," *Journal of Fluid Mechanics*, vol. 537, pp. 387–413, 2005.

[6] A. Zhang and Y. Liu, "Improved three-dimensional bubble dynamics model based on boundary element method," *Journal of Computational Physics*, vol. 294, pp. 208–223, 2015.

[7] S. Li, A. M. Zhang, R. Han, and Y. Q. Liu, "Experimental and numerical study on bubble-sphere interaction near a rigid wall," *Physics of Fluids*, vol. 29, no. 9, article 092102, 2017.

[8] Y. L. Liu, Q. X. Wang, S. P. Wang, and A. M. Zhang, "The motion of a 3D toroidal bubble and its interaction with a free surface near an inclined boundary," *Physics of Fluids*, vol. 28, no. 12, article 122101, 2016.

[9] A. M. Zhang, S. Li, and J. Cui, "Study on splitting of a toroidal bubble near a rigid boundary," *Physics of Fluids*, vol. 27, no. 6, article 062102, 2015.

[10] A. M. Zhang, W. B. Wu, Y. L. Liu, and Q. X. Wang, "Nonlinear interaction between underwater explosion bubble and structure based on fully coupled model," *Physics of Fluids*, vol. 29, no. 8, article 082111, 2017.

[11] R. H. Cole, *Underwater Explosions*, Princeton University Press, Princeton, NJ, USA, 1948.

[12] P. Cui, A. M. Zhang, and S. P. Wang, "Small-charge underwater explosion bubble experiments under various

boundary conditions," *Physics of Fluids*, vol. 28, no. 11, article 117103, 2016.

[13] J. M. Brett, G. Yiannakopoulos, and P. J. van der Schaaf, "Time-resolved measurement of the deformation of submerged cylinders subjected to loading from a nearby explosion," *International Journal of Impact Engineering*, vol. 24, no. 9, pp. 875–890, 2000.

[14] C. F. Hung and J. J. Hwangfu, "Experimental study of the behaviour of mini-charge underwater explosion bubbles near different boundaries," *Journal of Fluid Mechanics*, vol. 651, pp. 55–80, 2010.

[15] C. Hung, B. Lin, J. Hwang-Fuu, and P. Hsu, "Dynamic response of cylindrical shell structures subjected to underwater explosion," *Ocean Engineering*, vol. 36, no. 8, pp. 564–577, 2009.

[16] J. R. Krieger and G. L. Chahine, "Acoustic signals of underwater explosions near surfaces," *Journal of the Acoustical Society of America*, vol. 118, no. 5, pp. 2961–2974, 2005.

[17] Z. Fan, H. Ma, Z. Shen, and M. Lin, "Application of polyvinylidene fluoride for pressure measurements in an underwater explosion of aluminized explosives," *Combustion, Explosion, and Shock Waves*, vol. 51, no. 3, pp. 381–386, 2015.

[18] N. Li, J. Huang, K. Lei, J. Chen, and Q. Zhang, "The characteristic of the bubble generated by underwater high-voltage discharge," *Journal of Electrostatics*, vol. 69, no. 4, pp. 291–295, 2011.

[19] J. J. Lee, M. J. Smith, J. Huang, and G. T. Paulgaard, "Deformation and rupture of thin steel plates due to cumulative loading from underwater shock and bubble collapse," *Shock and Vibration*, vol. 18, no. 3, pp. 459–470, 2013.

[20] A. Jayaprakash, C.-T. Hsiao, and G. Chahine, "Numerical and experimental study of the interaction of a spark-generated bubble and a vertical wall," *Journal of Fluids Engineering*, vol. 134, no. 3, article 031301, 2012.

[21] S. Li, Y. Li, and A. Zhang, "Numerical analysis of the bubble jet impact on a rigid wall," *Applied Ocean Research*, vol. 50, pp. 227–236, 2015.

[22] S. Li, R. Han, A. Zhang, and Q. Wang, "Analysis of pressure field generated by a collapsing bubble," *Ocean Engineering*, vol. 117, pp. 22–38, 2016.

[23] L. Wang, Z. Zhang, and S. Wang, "Pressure characteristics of bubble collapse near a rigid wall in compressible fluid," *Applied Ocean Research*, vol. 59, pp. 183–192, 2016.

[24] E. Klaseboer, C. Turangan, S. W. Fong, T. G. Liu, K. C. Hung, and B. C. Khoo, "Simulations of pressure pulse-bubble interaction using boundary element method," *Computer Methods in Applied Mechanics and Engineering*, vol. 195, no. 33-36, pp. 4287–4302, 2006.

[25] B. Hopkinson, "A method of measuring the pressure produced in the detonation of high explosives or by the impact of bullets," *Philosophical Transactions of the Royal Society of London*, vol. 213, no. 612, pp. 437–456, 1914.

[26] H. Kolsky, "An investigation of the mechanical properties of materials at very high rates of loading," *Proceedings of the Physical Society. Section B*, vol. 62, no. 11, pp. 676–700, 1949.

[27] H. U. Leiste, *Experimental Studies to Investigate Pressure Loading on Target Plates*, Ph.D. thesis, Department of Mechanical Engineering, University of Maryland, College Park, MD, USA, 2012.

[28] S. E. Rigby, A. Tyas, S. D. Clarke et al., "Observations from preliminary experiments on spatial and temporal pressure measurements from near-field free air explosions," *International Journal of Protective Structures*, vol. 6, no. 2, pp. 175–190, 2015.

[29] S. D. Clarke, S. D. Fay, J. A. Warren, A. Tyas, S. E. Rigby, and I. Elgy, "A large scale experimental approach to the measurement of spatially and temporally localised loading from the detonation of shallow-buried explosives," *Measurement Science and Technology*, vol. 26, no. 1, article 015001, 2015.

[30] S. Clarke, S. Fay, J. Warren et al., "Predicting the role of geotechnical parameters on the output from shallow buried explosives," *International Journal of Impact Engineering*, vol. 102, pp. 117–128, 2017.

[31] S. E. Rigby, S. D. Fay, A. Tyas et al., "Influence of particle size distribution on the blast pressure profile from explosives buried in saturated soils," *Shock Waves*, vol. 28, no. 3, pp. 613–626, 2017.

[32] S. Rigby, S. Fay, S. Clarke et al., "Measuring spatial pressure distribution from explosives buried in dry Leighton Buzzard sand," *International Journal of Impact Engineering*, vol. 96, pp. 89–104, 2016.

[33] T. J. Cloete and G. N. Nurick, "Blast characterization using a ballistic pendulum with a centrally mounted hopkinson bar," *International Journal of Protective Structures*, vol. 7, no. 3, pp. 367–388, 2016.

[34] S. Park, T. Uth, N. Fleck, H. Wadley, and V. Deshpande, "Sand column impact onto a Kolsky pressure bar," *International Journal of Impact Engineering*, vol. 62, pp. 229–242, 2013.

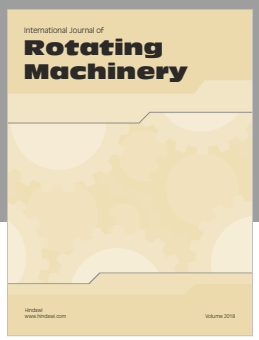

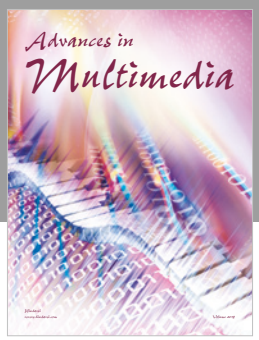

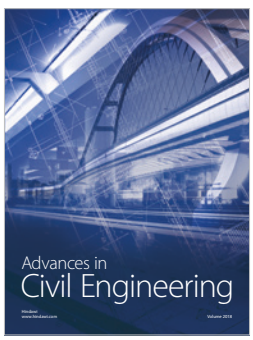

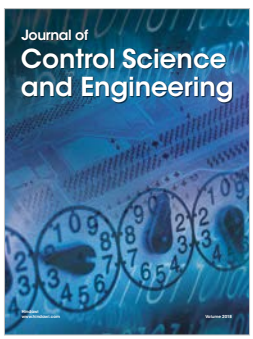

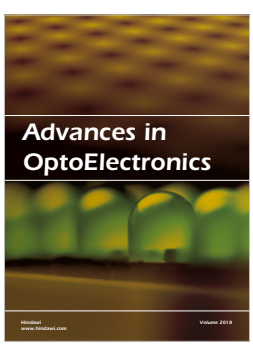

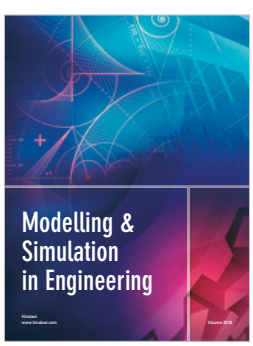

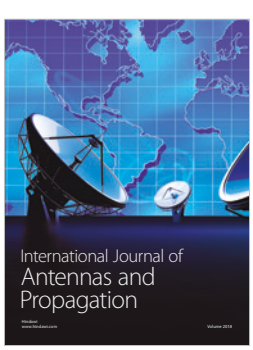

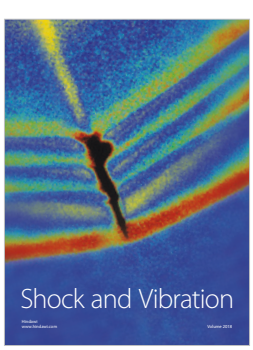

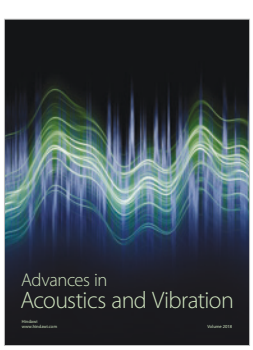

Hindawi

Submit your manuscripts at
www.hindawi.com